$Mn_{1-\ell}Cr_{\ell}As$ under pressure: Competition between magnetic orderings

A. Zięba
Institute of Physics and Nuclear Techniques, Academy of Mining and Metallurgy, 30059 Cracow, Poland

H. Fjellvåg and A. Kjekshus
Department of Chemistry, University of Oslo, N-0315 Oslo 3, Norway

R. Zach
Institute of Physics, Technical University of Cracow, 30084 Cracow, Poland
(Received 4 September 1990)

Pressure phase diagrams for the metallic magnet system $Mn_{1-\ell}Cr_{\ell}As$ are determined for $0.25 \leq \ell \leq 0.42$, $T > 77$ K, and $\mathcal{P} < 10$ kbar under fully hydrostatic conditions, and with a pressure resolution of 10^{-2} kbar. Three magnetically ordered phases [ferromagnetic F, helimagnetic H_c, and helimagnetic H_a (close to F in behavior)] exist within a certain, narrow $(\mathcal{P}, T, \ell)$ domain. The ordering temperatures of the F and H_a phases increase with pressure at a rate of up to 11 K/kbar. All the four possible types of triple points are experimentally studied. The H_a–F–P triple point is an approximate realization of a Lifshitz point, as verified by an incomplete divergence of the susceptibility on approaching the F phase. The H_c–F–P and H_c–H_a–P triple points show large umbilicuslike anomalies, qualitatively similar to those of bicritical points in the field phase diagrams of antiferromagnets.

I. INTRODUCTION

Experiments as well as spin-polarized band-structure calculations[1] indicate a general correlation between existence of magnetic moments and *increase* of unit-cell volume. An external pressure may, via lattice contraction, continuously change the magnetic properties and induce magnetic phase transitions. Such pressure effects are especially evident for 3*d* metal compounds, and result in part from their higher compressibility, as compared with the pure metals and their alloys. For the 3*d* metal monopnictides, all of which showing metallic properties, a clear correlation between the magnitude of the magnetic moment and increase in volume is found, whereas the actual types of crystal structure and of magnetic ordering appear to be of secondary importance.[2]

The pseudobinary MnAs–CrAs system is especially susceptible to the action of pressure in a region conveniently studied by the cylinder-piston technique. The magnetic properties of MnAs and CrAs are dramatically changed by relatively small pressures; MnAs undergoes a high- to low-spin transition at 4 kbar,[3] whereas for CrAs a pressure of 8 kbar completely destroys its magnetic moment.[4] For the $Mn_{1-t}Cr_tAs$ system, the situation is rather opposite. Some magnetically ordered phases are here favored by increased pressure due to an anomalous volume *decrease* during the ordering process.

The equilibrium phase diagram for well-annealed samples[5,6] of $Mn_{1-\ell}Cr_{\ell}As$ is shown in Fig. 1. The crystal structure is orthorhombic (*Pnma*). Three magnetically ordered phases are involved in the present pressure study. The H_a and H_c helimagnetic phases, of the double-spiral type,[5] are stable at ambient pressure. For the H_a ordering, the periodicity of the spirals amounts to a length of about $15a$ (≈ 85 Å).[5] Its behavior is close to ferromagnetic (F), and just a small critical field is required to align the magnetic moments.[6] The H_c phase is strongly antiferromagnetic, with critical fields exceeding at least 250 kOe.[6] The existence of a ferromagnetic phase under a pressure of some 5 kbar was first demonstrated by neu-

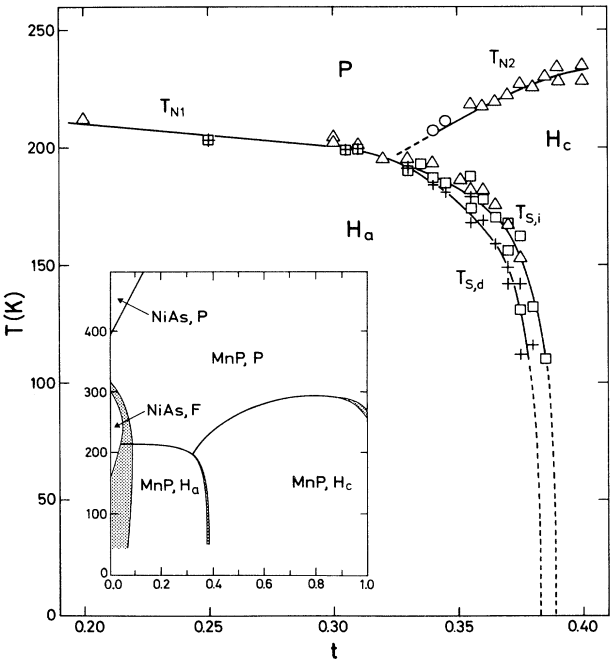

FIG. 1. Magnetic (ℓ, T) phase diagram of $Mn_{1-\ell}Cr_{\ell}As$, for $0.20 \leq \ell \leq 0.40$, quoted from Ref. 6. Magnetic phases are denoted F (ferromagnetic), H_a (a-axis helical), H_c (c-axis helical), and P (paramagnetic). Inset: magnetic and crystallographic phases (MnP or NiAs type) for the entire solid-solution phase $0 \leq \ell \leq 1$.

tron diffraction for $Mn_{0.615}Cr_{0.385}As$.[7] The F phase also occurs in the quatenary $Mn_{1-t}Ct_tAs_{1-x}P_x$ system[8] due to the chemical pressure generated by the nonmetal substitution.

The key difference between H_a, H_c, and F is probably not the geometrical arrangement of the magnetic moments, but rather distinctions in the electronic structures which are manifested as variations in the crystal lattice. The specific volume of the H_c phase is some 1% larger than that extrapolated from the paramagnetic phase,[6] whereas both H_a and F show an anomalous 2% decrease in volume.[6,8] As a consequence of the differences in volume, an external pressure should suppress the H_c phase and increase the domains of H_a and F. A decrease in volume at the disorder–order transition for H_a and F should be associated with positive $dT_{N1}/d\mathcal{P}$ and $dT_C/d\mathcal{P}$ slopes, which is quite an unusual situation for itinerant magnets [see, e.g., the compilation[9] of data for 25 itinerent ferromagnets which contain two examples (Ni and Sc_3In) with positive $dT_C/d\mathcal{P}$. Large positive slopes are also reported for the ferromagnet CoMnGe.[9]]

At ambient pressure, the H_a–H_c–P triple point occurs (Fig. 1), but the study of this requires a collection of samples, and this drawback clearly restricts a detailed investigation. Due to the existence of an F phase under pressure, other types of triple points, namely H_a–F–P, H_c–F–P, and H_a–H_c–F, should appear in some of the pressure–temperature phase diagrams. The main contribution of the present study is to map out such pressure–temperature phase diagrams with a pressure resolution of some 10^{-2} kbar. Careful searches are made for possible anomalies near the triple points. In particular, the pressure-induced H_a-to-F transition and the H_a–F–P triple point are studied and analyzed according to theories on helimagnetic order and multicritical behavior including Lifshitz points.

After this work had started, the somewhat differently aimed pressure study of Gribanov and Melnik[10] appeared, concerning the whole MnAs–CrAs system for pressures up to 30 kbar. The present work is focused on the composition range $0.25 < t < 0.43$, in which the competition of H_a, H_c, and F occurs at pressures below 10 kbars. Preliminary results of this work were presented at the International Conference on Magnetism 1988.[11]

II. EXPERIMENTAL METHODS

Polycrystalline samples of $Mn_{1-t}Cr_tAs$ were synthesized from MnAs and CrAs, as described in Ref. 5, in evacuated sealed silica-glass ampoules. The homogeneity and structural properties of the samples at ambient conditions were derived from powder x-ray diffraction measurements (Guinier camera, Cu$K\alpha_1$ radiation, Si as internal standard). The samples were further characterized by differential scanning calorimetry (DSC) measurements at temperatures between 100 and 900 K.

Pressures above ambient were generated inside a beryllium-brass pressure chamber connected to a 15-kbar helium-gas compressor (UNIPRESS, Warsaw) via a capillary tube. This gives *fully hydrostatic conditions* for the entire investigated pressure region (note that the helium is not frozen) and allows pressure tuning with a precision of 0.01 kbar. The apparatus allows both T=const and $\mathcal{P}$=const types of experimental runs. The temperature and pressure were measured using, respectively, a copper–constantan thermocouple and a manganin resistor. Phase transitions were detected via an ac susceptibility method. Contrary to the common practice, the ac field (300 Hz, few Oe) was generated by a coil surrounding the pressure chamber. The induced signal was detected by an axial three-section pick-up coil connected to a lock-in voltmeter. To ensure proper temperature homogeneity, the whole pressure chamber (with the sample and the coils) was subject to cooling by liquid nitrogen.

Figure 2 shows examples of the $\chi_{ac}(T)$ raw data curves recorded using a data-acquisition system,[12] based on an AMSTRAD CPC 6128 home computer. Measurements were performed for both increasing and decreasing temperature. During the measurements shown in Fig. 2, the pressure varied slightly, typically 0.01–0.06 kbar, due to

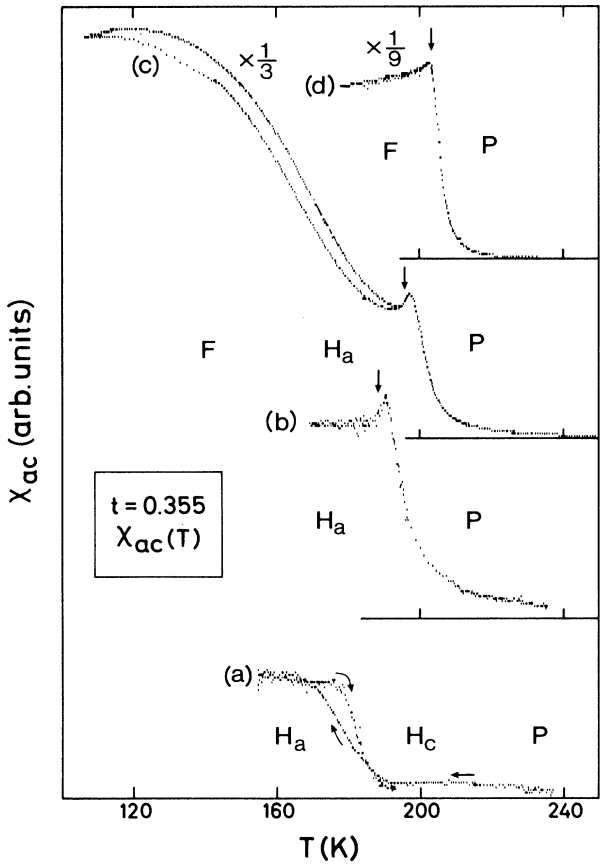

FIG. 2. Direct recordings of ac susceptibilities vs temperature for $Mn_{0.645}Cr_{0.355}As$ at (a) 0.3 kbar, (b) 1.1 kbar, (c) 1.94 kbar, and (d) 2.48 kbar. $\chi_{ac}(T)$ is recorded for decreasing and increasing temperature, measurement time 5 s per point. Symbols and arrows identify magnetic phases and location of transition temperatures, respectively.

expansion and contraction of the helium following the temperature change. The precision of the pressure measurements (about 0.01 kbar) is ruled by the hysteresis of the manganin pressure gauge and by the stability of the Wheatstone bridge.

The ac susceptibility curves for $Mn_{0.645}Cr_{0.355}As$ in Fig. 2 provides examples of four types of phase sequences: H_a to H_c (0.3 kbar), H_a to P (1.1 kbar), F to H_a and H_a to P (1.94 kbar), and F to P (2.48 kbar). Thermal hysteresis is recognized for some of the transitions. The H_c-to-F transition, which occurs for samples with higher ℓ, is also easily recognized (cf. Fig. 1 in Ref. 7) by this technique. However, the technique is not sensitive enough to detect the H_c-to-P transition.

The magnetic order–disorder temperatures T_{N1} (H_a to P) and T_C (F to P) were, respectively, taken as the inflection point slightly below the narrow maximum of the $\chi_{ac}(T)$ curves and as the extrapolated kink point (see Fig. 2). The temperatures of the weakly first-order transition T_{S1} (H_a to F) were taken as the inflection points, whereas the distinctly discontinuous transitions T_S (H_a to H_c) and T_{S2} (H_c to F) were taken as the midpoints of the susceptibility curves.

III. RESULTS

A. Phase diagrams

The pressure phase diagrams in Fig. 3 illustrate different topologies which appear depending on the sequence of magnetic phases at ambient pressure. $Mn_{0.75}Cr_{0.25}As$ is representative for the composition region $0.10 \leq \ell \leq 0.355$, where H_a is the only magnetically ordered phase at zero pressure. Consequently, a triple point between H_a, F, and P occurs under pressure. $Mn_{0.645}Cr_{0.355}As$ is representative for $0.335 \leq \ell \leq 0.385$, and the occurrence of two ordered phases at ambient pressure leads to the two triple points under pressure: H_c–H_a–P and H_a–F–P. Since the stability regions of H_c and F in the (P,T) phase diagrams increase with increasing Cr content at the expense of H_a, three triple points (the additional one being H_c–H_a–F) should exist in a narrow concentration range close to $\ell = 0.385$. The H_c–H_a–F point was observed in a sample prepared for neutron diffraction (ND) studies, $\ell = 0.39$ (ND), see Fig. 3(c), but no further emphasis was put on this noncritical triple point. The small-scale sample of $Mn_{0.61}Cr_{0.39}As$

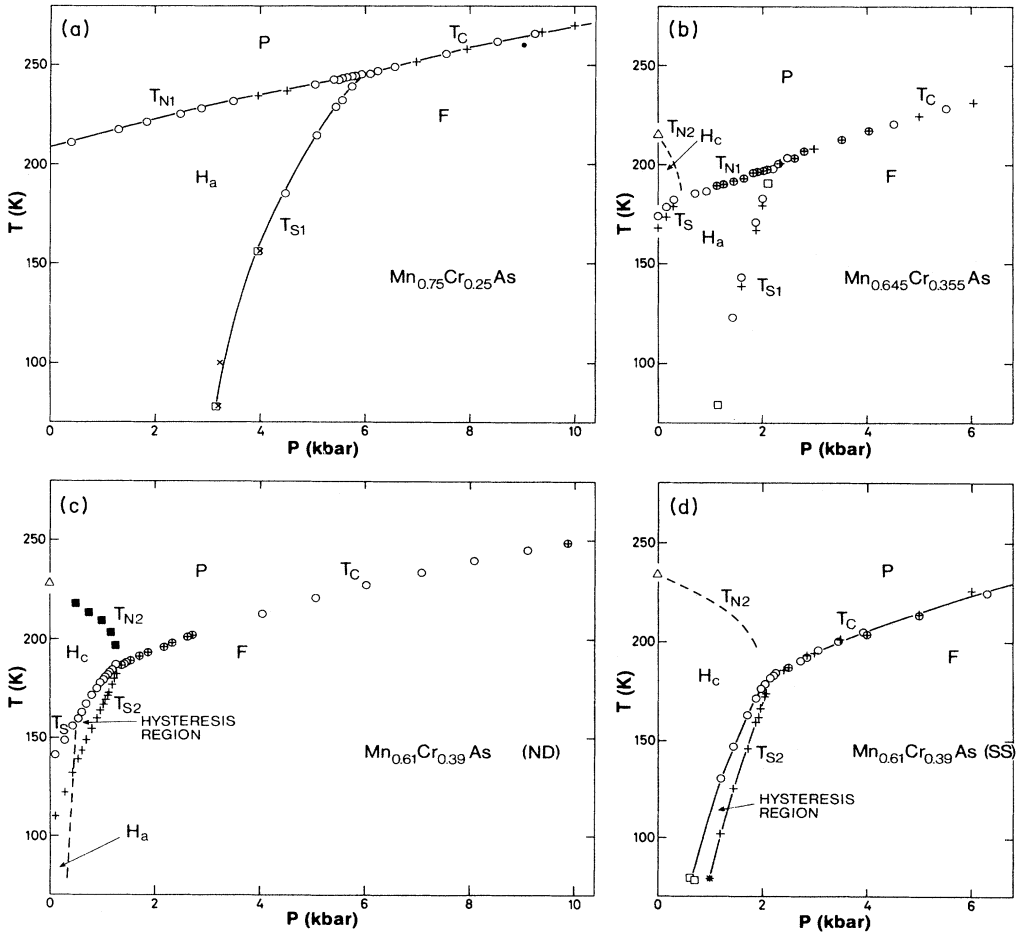

FIG. 3. Temperature–pressure phase diagrams for $Mn_{1-\ell}Cr_\ell As$; (a) $\ell = 0.250$, (b) $\ell = 0.355$, (c) $\ell = 0.39$ (ND), and (d) $\ell = 0.39$ (SS). Experimental points: ac susceptibility, $\mathcal{P}$=const runs, (○) heating and (+) cooling; T=const runs, (□) decreasing and (×) increasing pressure, (△) differential scanning calorimetry, (■) neutron diffraction from Ref. 13.

[marked SS in Fig. 3(d)] shows no H_a phase, however, in full accordance with the overall phase diagram in Fig. 1. Its $(\mathcal{P},T)$ phase diagram in Fig. 3(d) is representative for the chromium-rich part of the investigated system. Here H_c transforms directly to F. The coordinates of the H_c–F–P triple point for $t=0.39$ (SS), $\mathcal{P}=2.15$ kbar, and $T=170$ K, can be precisely deduced from the change in slope and the onset of temperature hysteresis for the phase boundaries surrounding the ferromagnetic phase. The observed difference for the two samples with the same nominal composition [a 20-g sample, $t=0.39$ (ND), and a 0.5-g sample, $t=0.39$ (SS)] is understandable since the H_c–H_a phase boundary in the (t,T) phase diagram (Fig. 1) is very steep and, consequently, susceptible to minute differences introduced through the preparation procedure.

The stability regions at liquid-nitrogen temperature for the different magnetic phases in the MnAs–CrAs system are shown in Fig. 4. Gribanov and Melnik[10] report surprisingly low P-to-F transition pressures for $t=0.55$ and 0.7, especially when confronted with the absence of ferromagnetism for $t=0.8$ and 0.9 (for $\mathcal{P}\leq 30$ kbar). The upper stability pressure of F remains an open problem that should be attacked by the diamond-anvil technique. Upon enhanced lattice compression, the magnetic moment must eventually collapse.

The H_a–F boundary extrapolates to $t=0.41\pm0.01$ at zero pressure (Fig. 4). This gives the upper limit for the stability of the H_a mode in $Mn_{1-t}Cr_tAs$ at ambient pressure in the absence of the competing H_c phase.

B. Magnetic order–disorder transitions

From the $(\mathcal{P},T)$ phase diagrams for $t=0.25$ and 0.355, it is seen that apart from possible anomalies very near the H_a–F–P triple points, the $T_{N1}(\mathcal{P})$ and $T_C(\mathcal{P})$ phase lines appear as one continuous phase boundary with a positive pressure slope. The dependencies $T_{N1}(\mathcal{P})$ and $T_C(\mathcal{P})$ are generally slightly nonlinear, with decreasing slope on increasing pressure. The maximum values of $dT_C/d\mathcal{P}$ near the triple points increase with increasing Cr content, being 7, 9, and 11 K/kbar for $t=0.25$, 0.355, and 0.39, respectively. Probably these pressure slopes actually represent the highest *positive* values found for magnetic order–disorder transitions, not only for itinerant ferromagnets, but in general.[9] This is also true when the slope is normalized to the Curie temperature. 11 K/kbar corresponds to $d\ln T_C/d\mathcal{P}=0.061$ kbar^{-1} and should, e.g., be compared to the otherwise highest values of 0.031 kbar^{-1} for Sc_3In and 0.011 kbar^{-1} for CoMnGe.[9] At high pressures, $T_C(\mathcal{P})$ tends to level off; nevertheless, $dT_C/d\mathcal{P}$ still remains very large. According to the data of Gribanov and Melnik[10] (for $t=0.15$ and 0.28), $T_C(\mathcal{P})$ becomes linear at pressures around 30 kbar with a slope of 3–4 K/kbar.

The susceptibility of the helimagnetic phase at the H_a–P transition grows on increasing the pressure towards the H_a–F–P triple point. This is manifested by an increasing peak in the ac susceptibility close to the Néel point (compare the curves for 1.1 and 1.94 kbar in Fig. 2). The pressure dependencies of the χ_{ac} peak value close to T_{N1}, i.e., along the $T_{N1}(\mathcal{P})$ line, and of the extrapolated $\chi_{ac}(T)$ kink point are shown in Fig. 5 for $t=0.355$. The susceptibilities are normalized to the

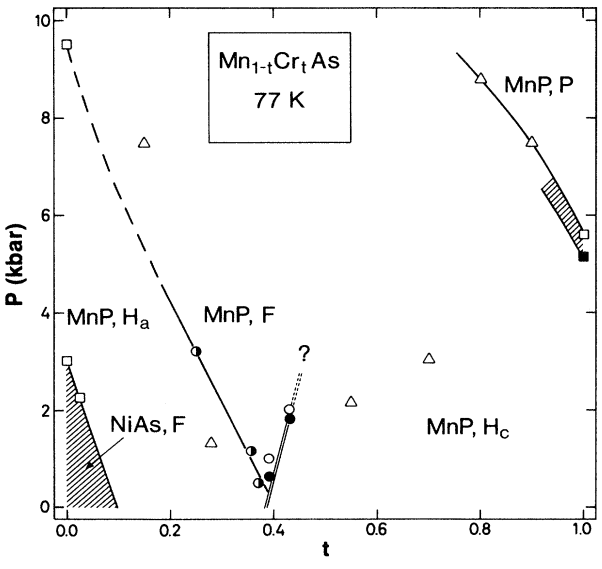

FIG. 4. Composition–pressure phase diagram for $Mn_{1-t}Cr_tAs$ at $T\approx 77$ K. Experimental points: (○,●) this work, (△) Gribanov and Melnik (Ref. 10), and (□,■) from Refs. 3, 4, and 14. Open and solid symbols denote increasing and decreasing pressure or temperature conditions, respectively.

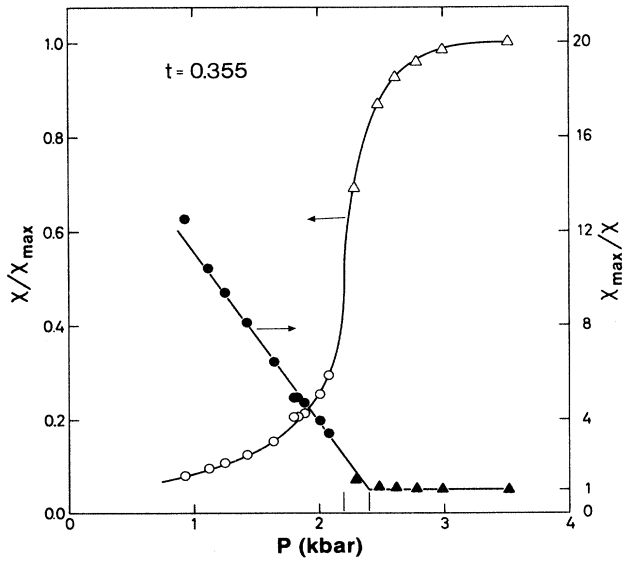

FIG. 5. Variations of normalized ac magnetic susceptibility (open symbols, χ/χ_{max}) and its inverse (filled symbols, χ_{max}/χ) along the critical phase boundary for $Mn_{0.645}Cr_{0.355}As$. Circles correspond to χ_{ac} peak just above T_{N1}, and triangles to kink point at T_C.

maximum value, χ_{max}, of the F phase (limited by demagnetization). Figure 5 shows that χ_{max}/χ decreases approximately linearly on approaching the triple point, but extrapolates to 1 (i.e., to zero for the true susceptibility not limited by demagnetization) at a pressure of about 0.2 kbar above the observed triple point.

The pressure slope for the H_c-to-P phase boundary is, on the other hand, negative and also exceptionally steep. This can be judged by considering the $T_{N2}(\mathcal{P})$ phase line, which connects the H_c-H_a(or $-F$)$-P$ triple point and T_{N2} at zero pressure, cf. the dashed curves in Figs. 3(b) and 3(d). The $T_{N2}(\mathcal{P})$ boundary, as determined by neutron diffraction[13] [Fig. 3(c)], is distinctly nonlinear, with a slope of roughly -15 K/kbar at ambient pressure, whereas the boundary becomes practically vertical on approaching the triple point. This observation is consistent with the study of Gribanov and Melnik.[10]

C. Magnetic order–order transitions

At ambient pressure, only one transition occurs between ordered phases, viz., the H_a-to-H_c transition. Under pressure, additional transitions of this category appear due to the occurrence of the F phase.

The similarity in the nature of H_a and F makes the first-order T_{S1} transition relatively weak. This is supported experimentally by the small-pressure hysteresis of about 0.05 kbar (from T=const runs), which is fully consistent with the larger temperature hysteresis of 9 K (see curve for 1.94 kbar in Fig. 2) when one takes into account the steepness of the $T_{S1}(\mathcal{P})$ line. The latent heat of the H_a-F transition can be determined indirectly. For $t=0.355$ (at 80 K), $dT_{S1}/d\mathcal{P}$ is 110 K/kbar. Results for the field-induced H_a-to-F transition (also at 80 K); see Fig. 2 of Ref. 11) implies that $d\mathcal{H}/d\mathcal{P}=0.43$ T/kbar. From the thermodynamic relations $d\mathcal{H}/d\mathcal{P}=\Delta\mathcal{M}/\Delta\mathcal{V}$ ($\Delta\mathcal{M}$ being the jump in magnetization) and $dT/d\mathcal{P}=T\,\Delta\mathcal{V}/Q$, a latent heat of $Q=0.02$ J/g and a relative jump in unit cell volume of $\Delta\mathcal{V}/\mathcal{V}=0.2\%$ are estimated.

The heat-capacity measurement by Labban *et al.*[15] in the region of the T_{S1} transition for the isostructural $MnAs_{0.88}P_{0.12}$ phase, shows only a minute anomaly, but no value for the very small latent heat was given. No volume jump could be established by powder diffraction. Similar observations are made for the helimagnetic-to-ferromagnetic transition of the MnP prototype. Also here $\Delta\mathcal{V}$ is extremely small, however, with jumps $<0.1\%$ in the individual unit cell parameters (positive and negative).[16] Further considerations on the nature of the H_a-to-F transition are given in Sec. IV.

All observations indicate that the H_c-to-F transition is of larger "strength." A value for $d\mathcal{H}/d\mathcal{P}$ can be obtained from the pressure and field phase diagrams for $t=0.39$ (see Sec. IV). Using the same thermodynamic relations as above, the volume jump for the H_c-to-F transition is estimated to 3%, and the latent heat to 0.3 J/g at 80 K. The large $\Delta\mathcal{V}/\mathcal{V}$ is fully consistent with the change in the unit-cell dimensions that occur at ambient pressure in $Mn_{1-t}Cr_tAs$ on passing from H_a to H_c at low temperatures (about 3.2% at 10 K independent of t, see Fig. 4 of Ref. 6; note that H_a and F have approxi-

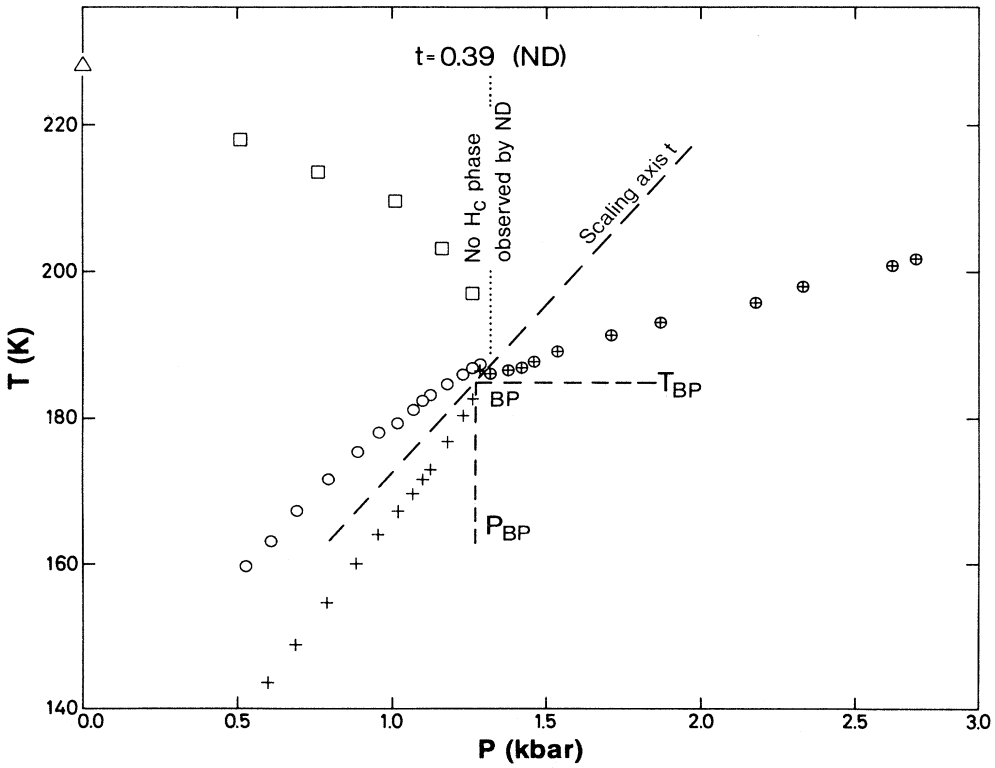

FIG. 6. $(\mathcal{P},T)$ phase diagram for $Mn_{0.61}Cr_{0.39}As$ (ND) in vicinity of H_c-F-P triple point [see text and Fig. 3(c)].

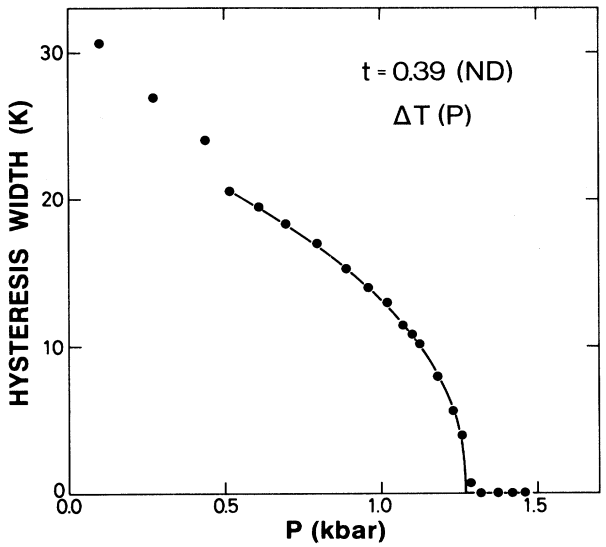

FIG. 7. Pressure dependence of hysteresis width for $\ell=0.395$ (ND). Solid line represents exponential fit to data, see Sec. IV B.

mately equal unit-cell volumes).

The distinct first-order character of the H_c-to-F transition is also testified by large hysteresis, and, e.g., for $\ell=0.39$ (ND), $\Delta\mathcal{P}$ amounts to 0.4 kbar at low temperature (Fig. 6). The hysteresis decreases rapidly to zero at the H_c-F-P triple point. In Ref. 11 this was suggested to occur discontinuously. However, the more precise data presented in Fig. 7 suggest a steep, continuous decrease of the thermal hysteresis, perhaps described by some power law. Extrapolation of the $\Delta T(\mathcal{P})$ curve to zero allows precise determination of the pressure coordinate of the H_c-F-P triple point to $\mathcal{P}=1.27\pm0.02$ kbar. The marked increase of the hysteresis at $\mathcal{P}=0.47\pm0.3$ kbar (Fig. 7) locates the noncritical H_c-H_a-F triple point.

IV. DISCUSSION

A. Weakly discontinuous helimagnetic H_a to ferromagnetic F transition and character of the H_a-F-P triple point

The similarity of the H_a and F phases suggests that both types of ordering, and in consequence also the helimagnetic-to-ferromagnetic transition, can be described in terms of a localized spin model by the same set of exchange parameters.

The helimagnetic H_a structure has some common features with the H_c structure in MnP and is of the double-screw type with four magnetic atoms in the crystallographic unit cell. To explain the stability of the H_c structure of MnP, no less than five exchange parameters are required.[17] However, the essential physics of the helimagnetic-to-ferromagnetic transition in MnP is accounted for by the classical Hamiltonian for N spins per unit volume confined to parallel planes with ferromagnetic coupling ($\mathcal{J}_1>0$) between the spins of neighboring planes and antiferromagnetic coupling ($\mathcal{J}_2<0$) between next-neighboring planes, together with terms describing the orthorhombic magnetocrystalline anisotropy. In an approximate description, the H_a spiral propagates along **a** with spins ferromagnetically coupled within *bc* planes that are $a/2$ apart. For MnP, this model was used to account for the magnetic properties at low temperature,[18] for discussing the helimagnetic–ferromagnetic transition at 47 K,[19] and for explaining the Lifshitz point in the magnetic phase diagrams.[20] In the absence of anisotropy, the ferromagnetic phase is stable for $\mathcal{J}_2/\mathcal{J}_1>-\frac{1}{4}$, otherwise the helimagnetic mode occurs with a pitch angle (Θ) given as

$$\cos\Theta=-\mathcal{J}_1/4\mathcal{J}_2 \ . \tag{1}$$

The helimagnetic–ferromagnetic boundary is then of second order. Θ goes to zero, and the in-plane magnetic susceptibility diverges on approaching the transition. In the mean-field approximation (MFA), Eq. (1) is valid at any temperature implying a vertical $H-F$ boundary in the temperature versus $\mathcal{J}_2/\mathcal{J}_1$ phase diagram. The $H-F$ boundary terminates in the $H-F-P$ triple point with Lifshitz character. The effect of critical fluctuations is to extend the area of the F phase at high temperatures. Calculations by Redner and Stanley,[21] using high-temperature series expansion (HTSE), tell that at $T=0$ K, the $H-P$ boundary starts at $\mathcal{J}_2/\mathcal{J}_1=-0.25$ and hits the Lifshitz point for $\mathcal{J}_2/\mathcal{J}_1=-0.263\pm0.002$ and -0.259 ± 0.002 for order-parameter dimensionalities $n=2$ and 3, respectively (cf. Ref. 21).

In the presence of anisotropy, the $H-F$ transition becomes first order. The energy of the system is reduced by discontinuously switching the spins of the long spiral into the (ferromagnetic) easy direction. The F domain thereby becomes extended (Fig. 6). Another source for turning the transition discontinuous, is the magnetocrystalline coupling, which in localized-moment models is required to account for jumps in the unit-cell dimensions. According to mean-field calculations, already an arbitrary small coupling turns the $H-F$ transition into first order.[22] This is in contrast to the $F-P$ transition, which becomes discontinuous only if the coupling exceeds some threshold value.[23] (Modern theories predict a fluctuation-driven discontinuity for an arbitrary small coupling, but it is believed that the effect is so small that it escapes detection.)

The experimental data comply qualitatively with the theory outlined above. Equation (1) suggests that small changes in the exchange constants are sufficient to produce large variations in the angle Θ. For example, for $\ell=0.25$, the low-temperature value[5] $\Theta=17°$ is reduced to 0° at 3 kbar, whereas $\mathcal{J}_2/\mathcal{J}_1$ changes merely from -0.263 to -0.25. Such a small change cannot produce any larger variation in the transition temperature on going from T_C to T_{N1}. Consequently, on a large scale, the T_{N1} boundary is almost an extension of $T_C(\mathcal{P})$, but shows an upward tendency as expected from theory.[21]

The $T_{S1}(\mathcal{P})$ boundary for, e.g., $Mn_{0.75}Cr_{0.25}As$ [Fig. 3(a)] shows an apparent disagreement with theory in that

the domain of the H phase, rather than that of F, grows on approaching the critical line. This is probably due to the thermal expansion of the structure, which opposes the contraction forced by the applied external pressure. It is reasonable to assume that $\mathcal{J}_2/\mathcal{J}_1$ is a function of interatomic distances instead of pressure alone. An estimate, based on the observed thermal expansion and a compressibility of 2×10^{-3} K/kbar estimated from data for CrAs and MnAs (Ref. 24) brings the $T_{S1}(\mathcal{P})$ line, perhaps accidentally, in accord with the HTSE calculations.

The incomplete divergence of the magnetic susceptibility along the T_{N1} boundary clearly supports the closeness to Lifshitz-like behavior of the system. The data suggest that, in the absence of anisotropy, the real Lifshitz point should be located at a pressure some 0.2 kbar higher than the observed H_a-F-P triple point. A confirmation of the nature of the phase diagram calls for determination of the modulation vector as a function of T and $\mathcal{P}$ by neutron diffraction.

Finally, the attention is paid to the possible anomalies of T_{N1} and T_C near the triple point. The applied helium-gas-compression technique provides a considerably better pressure resolution and tunability than methods used in earlier studies of pressure phase diagrams of magnetic materials with triple points.[25–28] Inspection of the $(\mathcal{P},T)$ phase diagrams for $t=0.25$ and 0.355 (Fig. 3) suggests about a 2-K deep umbilicuslike anomaly. Such an anomaly is not inconsistent with theory, because on a small pressure scale, the H_a-F-P triple point should become a bicritical point. The experimental evidences are, however, inconclusive because of problems with reliable determination of the exact transition temperatures. T_{N1} is derived from the inflection point of $\chi_{ac}(T)$, which is some 1–2 K below the peak position, and it may be influenced by minor, nevertheless always present, inhomogeneities in the samples. When the extrapolated kink point is used to assess the Curie temperature, any inhomogeneity will cause a lowering of the transition temperature. In particular, the various criteria are difficult to apply close to the triple point.

B. Comparison between helimagnetic H_c and ferromagnetic F phases and character of H_c-F-P triple point

An appropriate question concerning the H_c-to-P and the F-to-P transitions is why the corresponding pressure derivatives are so high. The high values for $dT_C/d\mathcal{P}$ for $Mn_{1-t}Cr_tAs$ are the highest known. However, the facts that $|dT_{N2}/d\mathcal{P}|$ is even higher and that T_{N2} neighbors the T_C boundary in the $(\mathcal{P},T)$ space are probably not incidental. The pressure dependencies of both boundaries are nonlinear (Figs. 3, 6, and 7). The curvatures of $T_{N2}(\mathcal{P})$ and $T_C(\mathcal{P})$ increase on approaching the triple point. The decrease of the ordering temperature for one phase on approaching the triple point seems influenced by the "proximity" of the second, competing phase. These large (positive or negative) pressure derivatives of the magnetic order–disorder temperatures are difficult to reconcile within the MFA theory on magnetoelastic coupling.[23] Such models predict the transitions to be discontinuous when the pressure derivatives are as large as observed in the present case.[29] The classical approximation is very crude; nevertheless, it describes well the properties of the binary end phases, MnAs and CrAs, of the $Mn_{1-t}Cr_tAs$ solid-solution phase. For MnAs and CrAs, large negative pressure derivatives are connected with a discontinuous character of the transition to the paramagnetic phase. We believe that the extraordinary behavior of the phase boundaries around the H_c-F-P triple point indicate that this point rather has a *bicritical* nature with a very large range of bicritical behavior.

The bicritical point concerns the situation where a disordered phase may transform, via second-order transitions, into two different ordered phases. According to mean-field theory, the phase boundaries cross each other at sharp angles. The effect of critical fluctuations is well established, both experimentally[30,31] and theoretically,[32,33] for bicritical points in the phase diagrams of antiferromagnets in external magnetic field. The fluctuations cause the critical phase boundaries to become nonlinear, and joined tangentially to the first-order boundary at the bicritical point (BP). Their shape in the vicinity of BP (scaling axes g,t centered at BP) is according to the generalized scaling hypothesis

$$g=\omega_{1,2}t^{\phi}\ , \tag{2}$$

where the amplitude ratio $\omega_{1,2}=\omega_1/\omega_2$ and the crossover exponent ϕ are universal quantities dependent on the system symmetry and the order-parameters dimensionalities n_1 or n_2 for the competing antiferromagnetic (AF) and spin-flop phases. For large values of $n_{BP}=n_1+n_2$, theory predicts[32] a decoupled tetracritical point with, again, critical lines crossing at distinct angles.

Contrary to the universal quantities connected to the BP situation, the question of magnitude has received little attention. The magnitude of the effect can tentatively be defined as the difference between the temperature coordinate for the bicritical point, T_{BP}, and the temperature T^*_{BP} obtained by extrapolation of the phase boundaries from a region far from BP. The experimental data for BP's of antiferromagnets (see the review in Ref. 31) show that the magnitude is small and strongly correlated with n_{BP}. $(T^*_{BP}-T_{BP})/T_{BP}$ equals 0.03 for $GaAlO_3$,[30] which is typical for $n_{BP}=2$. However, this ratio becomes more than an order of magnitude smaller for BP's with $n_{BP}=3$.

The pressure phase diagram for $t=0.39$ (ND) is in the vicinity of the H_c-F-P triple point, qualitatively resembling the $(\mathcal{H}^2,T)$ diagrams for $GaAlO_3$ and MnF_2 (H_c and F corresponding, respectively, to spin-flop and AF phases), but with the magnitude of the anomalous region being much larger. The value for $(T^*_{BP}-T_{BP})/T_{BP}$ for $t=0.39$ is at least 0.10.

Attempts were made to check the possible bicritical scaling according to Eq. (2). The scaling axis t was fitted to the midpoints (for $\mathcal{P}>1.3$ kbar) of the hysteresis region (Fig. 6). This was motivated by the fact that the mean values of T_{S2} for heating and cooling show an approximately linear pressure dependence, whereas the T_{S2} thermodynamic equilibrium line is unknown. Rather

surprisingly, the pressure dependence of the thermal hysteresis is well described by the power law $\Delta T \propto (\mathcal{P}_{BP}-\mathcal{P})^{\tau}$, with $\mathcal{P}_{BP}=1.27$ kbar, and $\tau=0.44(1)$. At $\mathcal{P}_{BP}$ the corresponding temperature value on the g line is $T_{BP}=184.8$ K. Hence, the coordinates of BP and one of the scaling axis can be established without utilizing data from the critical phase boundaries. The inclination of the t scaling axis may, in the same way as for the H_a-F-P triple point, result from the interplay between thermal expansion and pressure contraction.

The whole $T_C(\mathcal{P})$ up to 10 kbar and also the less accurately known $T_{N2}(\mathcal{P})$ are, on the other hand, not well described by Eq. (2). However, if one limits the consideration to $t<0.1$ and applies fit to the $T_C(\mathcal{P})$ data alone (Fig. 7), the exponent ϕ becomes 1.27(5) under the assumption that the second scaling axis g is horizontal. Unfortunately, the data for $T_{N2}(\mathcal{P})$ are not precise enough to test the crucial content of the generalized scaling, which implies that *both* critical lines are to be described by the same exponent.

The results concerning the BP in $Mn_{1-t}Cr_tAs$ partly contradict expectations based on theory. This may possibly be traced to the itinerant nature of the magnetic phases involved.[34] Contrary to the case of localized magnetism, the amplitude of the local "moments" in itinerant systems also fluctuates, and it is possible for the ordering temperature to go to zero with still large "moments" in the paramagnetic state. However, the very concept of the BP order-parameter dimensionality may be invalid because the simultaneous existence of "moments" of both phases, linked to the different band structures, is at least limited. One may speculate whether massive short-range order, as accounted for by fluctuation band theories,[34] but not by localized-moment systems, is responsible for anomalies in the phase boundaries at large values of the reduced temperature.

The H_c and F phases differ by as much as 3% in unit-cell volume. Fluctuations of the moment in the bicritical region should hence be coupled to fluctuations in density. This should lead to a large compressibility in the bicritical region, easily detectable by x-ray or neutron diffraction under pressure (for preliminary results, see Ref. 13).

Only a few examples of pressure phase diagrams including an AF–F–P triple point[25–27] are known. All of these were studied using pressurized clamps with rather imprecise tuning and measuring of the pressure. The best example of a bicritical point in such $(\mathcal{P},T)$ phase diagrams may be provided by the cubic, localized spin compound EuSe, of which the antiferromagnetic phase with $n_1=8$ transforms into a ferromagnetic phase with $n_2=3$ at 5 kbar.[28] For such dimensions, the theory predicts no anomaly, and this is consistent with the (rather imprecise) experimental phase diagram.[25] It would be interesting to reexamine itinerant-moment systems, such as $Hf_{1-x}Ta_xFe_2$ and Fe_2P, for which existing data[27,25] provide indications for anomalies near the F–AF–P triple point.

The bicritical H_c-F-P point in $Mn_{1-t}Cr_tAs$ has another interesting feature; the field conjugate to the order parameter of one of the competing phases (i.e., F) exists physically. Figure 8 shows, using the experimental data for the $t=0.39$ (SS) sample, a sketch of the three-dimensional $(\mathcal{H},\mathcal{P},T)$ phase diagram. The domain of the ordered (H_c) phase, which is not conjugated to the field, is limited by the surface defined by the first- and second-order lines connected along the tricritical line originating at BP. This type of topology was first discussed by Kosterlitz[32] for a uniaxial antiferromagnet, for which there is no physical realization of the staggered field.

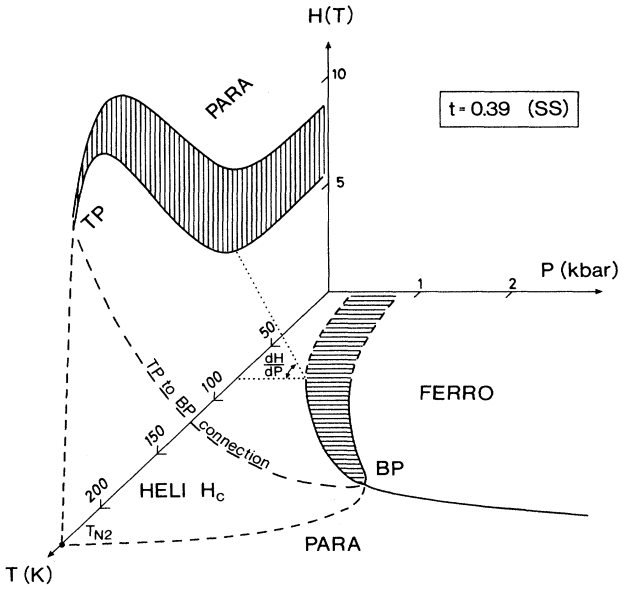

FIG. 8. Schematic pressure–field–temperature phase diagram for $t=0.39$ (SS). Solid curves are based on experimental data given in Ref. 6 and this work.

V. CONCLUSIONS

The pressure diagrams of $Mn_{1-t}Cr_tAs$, with $0.25 \le t \le 0.42$, show all four types of triple points that appear in a system with three ordered and one disordered magnetic phase. The phase diagrams are in the vicinity of the triple points determined with a precision up to 0.01 kbar, which is considerably better than other $(\mathcal{P},T)$ phase diagrams thus far reported for magnetic systems. This was made possible by the use of helium as the pressure-transmitting medium, since the triple points appear in a region where helium is not frozen.

The present study provides *inter alia* results on two different cases of magnetic competition and corresponding multicritical behavior. The pressure-induced transition from the H_a helimagnetic phase (with long periodicity) to ferromagnetism appears as weakly discontinuous. The incomplete divergence of the susceptibility along the $T_{N1}(\mathcal{P})$ line on approaching the H_a-F-P triple point suggests that this triple point exhibits the characteristics of a Lifshitz point on a large pressure scale. The shapes of the phase boundaries are in qualitative agreement with (ANNI XY or Heisenberg) model predictions when the effect of thermal expansion of the lattice is also taken into account.

The most striking feature of the H_c–F–P triple point is the anomalous decrease of ordering temperatures for the competing H_c and F phases over a large interval around the triple point. The anomaly can be expressed in terms of very large pressure derivatives. In fact, $dT_C/d\mathcal{P}=11$ K/kbar appears to represent the highest value known thus far. Near the triple point, the phase boundaries show resemblance to the well-known bicritical point in the field diagrams of anisotropic antiferromagnets. The experimental data provides a check on the applicability of the generalized scaling concept. The "bicritical H_c–F–P point" cannot directly be described by existing theories on bicritical behavior, a feature that is believed to originate from the itinerent nature of both of the competing magnetic phases.

ACKNOWLEDGMENTS

The cooperation of T. Chattopadhyay, P. Karen, and C. Vettier in collecting the neutron-diffraction data in Ref. 13 is gratefully acknowledged. This work was supported by the Norwegian Research Council for Science and the Humanities and by the Polish Academy of Sciences Grant No. CPBP.01.12.

[1]V. L. Moruzzi, J. F. Janak, and A. R. Williams, *Calculated Electronic Properties of Metals* (Pergamon, New York, 1978).
[2]H. Fjellvåg, A. Kjekshus, A. F. Andresen, and A. Zięba, J. Magn. Magn. Mater. **61**, 61 (1986).
[3]N. Menyuk, J. A. Kafalas, K. Dwight, and J. B. Goodenough, Phys. Rev. **177**, 942 (1969).
[4]E. A. Zavadskii and I. A. Sibarova, Zh. Eksp. Teor. Fiz. **78**, 1076 (1980) [Sov. Phys. JETP **51**, 542 (1980)].
[5]H. Fjellvåg and A. Kjekshus, Acta. Chem. Scand. Ser. A **38**, 1 (1984); **39**, 671 (1985).
[6]A. Zięba, H. Fjellvåg, and A. Kjekshus, J. Magn. Magn. Mater. **68**, 115 (1987).
[7]A. F. Andresen, H. Fjellvåg, A. Kjekshus, and B. Lebech, J. Magn. Magn. Mater. **62**, 247 (1986).
[8]A. F. Andresen, K. Bärner, H. Fjellvåg, A. Kjekshus, H. Rager, U. Sondermann, and S. Stølen, J. Magn. Magn. Mater. **94**, 347 (1991).
[9]J. Inoue and M. Shimitzu, Phys. Lett. **90A**, 85 (1982); S. Niziol, A. Zięba, R. Zach, R. Baj, and K. Dmowski, J. Magn. Magn. Mater. **38**, 205 (1983).
[10]I. F. Gribanov and V. A. Melnik, J. Magn. Magn. Mater. **71**, 219 (1988).
[11]A. Zięba, R. Zach, H. Fjellvåg, and A. Kjekshus, J. Phys. (Paris) Colloq. Suppl. **12**, C8-203 (1988).
[12]P. Grodzinski, J. Swakon, and A. Zięba, IFTJ, Report No. INT 229/PS, 1988 (unpublished).
[13]H. Fjellvåg, P. Karen, A. Kjekshus, A. Zięba, T. Chattopadhyay, and C. Vettier, J. Magn. Magn. Mater. **92**, 75 (1990).
[14]A. Zięba, R. Zach, H. Fjellvåg, and A. Kjekshus, J. Phys. Chem. Solids **48**, 79 (1987).
[15]A. K. Labban, E. F. Westrum, Jr., H. Fjellvåg, F. Grønvold, A. Kjekshus, and S. Stølen, J. Solid State Chem. **70**, 185 (1987).
[16]T. Okamoto, T. Kamigaichi, N. Iwata, and E. Tatsumoto, J. Phys. Soc. Jpn. **25**, 1730 (1968); A. Ishizaki, T. Komatsubara, and E. Hirahara, *ibid.* **30**, 292 (1971).
[17]L. Dobrzynski and A. F. Andresen, J. Magn. Magn. Mater. **82**, 67 (1989).
[18]S. Hiyamitzu and T. Nagamiya, Int. J. Magn. **2**, 33 (1972).
[19]J. Smit, Solid State Commun. **477**, 87 (1983).
[20]C. S. O. Yokoi, M. D. Countinho-Filho, and S. R. Salinas, Phys. Rev. B **24**, 5430 (1981).
[21]S. Render and H. E. Stanley, Phys. Rev. B **16**, 4901 (1977).
[22]A. Zięba (unpublished).
[23]C. P. Bean and D. S. Rodbell, Phys. Rev. **126**, 104 (1962).
[24]V. I. Kamenev and E. A. Zavadskii, Fiz. Tverd. Tela (Leningrad) **20**, 933 (1978); N. N. Sirota, E. A. Vasilev, and G. A. Govor, J. Phys. (Paris) Colloq. **32**, C1-1987 (1971).
[25]H. Fujiwara, Physica B+C **119B**, 142 (1983).
[26]E. M. Gyorgy, B. Batlogg, J. P. Remeika, R. B. van Dover, R. M. Fleming, H. E. Bair, G. P. Espinosa, A. S. Cooper, and R. G. Maines, J. Appl. Phys. **61**, 4237 (1987).
[27]K. Hoshi, H. Kiya, N. Mori, Y. Nishihara, and Y. Yamaguchi, J. Phys. Soc. Jpn. **54**, 3683 (1985).
[28]K. Westerholt and T. Wegmann, Phys. Rev. B **35**, 7287 (1987).
[29]For the isotropic ferromagnet the transition becomes first order for $\eta=\frac{3}{2}(Nk_B/T_CK)|dT_C/d\mathcal{P}|^2>1$, where N is the number of one-half spins, k_B the Boltzmann constant, and K the compressibility. Assuming (Ref. 24) that $K=3\times10^{-3}$ kbar^{-1}, one obtains $\eta=1.4$ for a derivative of 11 K/kbar, and still larger η for the T_{N2} phase boundary.
[30]H. Rohrer, Phys. Rev. Lett. **34**, 1638 (1975).
[31]Y. Shapira, in *Multicritical Phenomena,* edited by R. Pynn and A. Skjeltorp (Plenum, New York, London, 1984).
[32]J. M. Kosterlitz, D. R. Nelson, and M. E. Fisher, Phys. Rev. B **13**, 412 (1976).
[33]A. D. Bruce and A. Aharony, Phys. Rev. B **11**, 478 (1975).
[34]H. Cappellmann, *Metallic Magnetism* (Springer, Berlin, 1986).